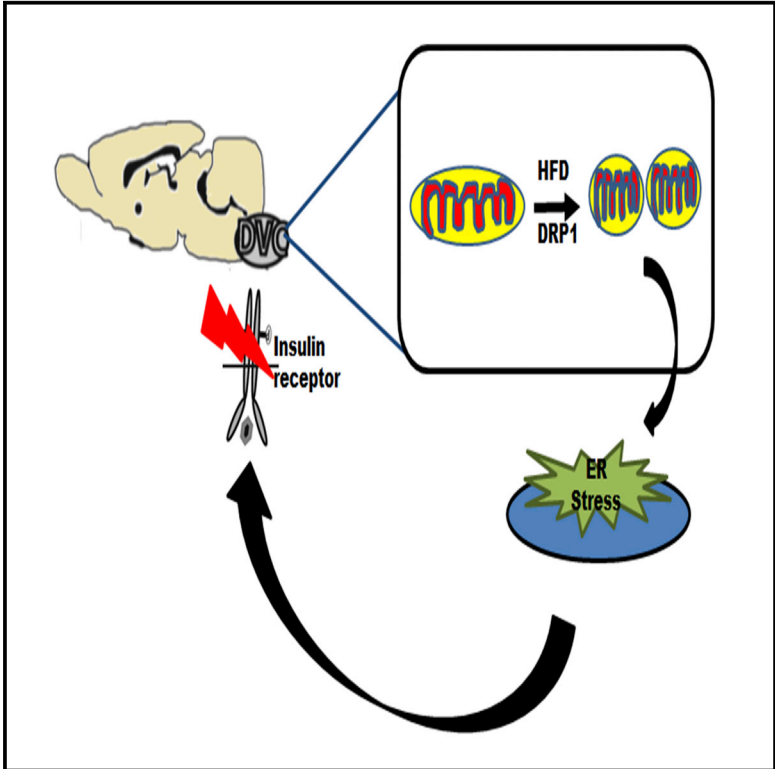


Dynamin-Related Protein 1-Dependent Mitochondrial Fission Changes in the Dorsal Vagal Complex Regulate Insulin Action

Graphical Abstract



Authors

Beatrice M. Filippi, Mona A. Abraham, Pamuditha N. Silva, ..., Paige V. Bauer, Jonathan V. Rocheleau, Tony K.T. Lam

Correspondence

tony.lam@uhnres.utoronto.ca

In Brief

Filippi et al. find that induction of Drp1-dependent mitochondrial fission in the dorsal vagal complex of rodents under high-fat feeding can induce ER stress and insulin resistance.

Highlights

- HFD induces Drp1-dependent mitochondrial fission in the rodent DVC
- Drp1-mitochondrial fission inhibition reverses HFD-induced insulin resistance
- Drp1-mitochondrial fission alone induces insulin resistance in healthy rodents
- Drp1-mitochondrial fission induces ER-stress-dependent insulin resistance



Dynamin-Related Protein 1-Dependent Mitochondrial Fission Changes in the Dorsal Vagal Complex Regulate Insulin Action

Beatrice M. Filippi,^{1,6,7} Mona A. Abraham,^{1,2,6} Pamuditha N. Silva,³ Mozhgan Rasti,¹ Mary P. LaPierre,^{1,2} Paige V. Bauer,^{1,2} Jonathan V. Rocheleau,^{1,2,3,4,5} and Tony K.T. Lam^{1,2,4,5,8,*}

¹Toronto General Hospital Research Institute and Department of Medicine, UHN, Toronto, ON M5G 1L7, Canada

²Department of Physiology, University of Toronto, Toronto, ON M5S 1A8, Canada

³Institute of Biomaterials and Biomedical Engineering, University of Toronto, Toronto, ON M5S 3G9, Canada

⁴Department of Medicine, University of Toronto, Toronto, ON M5S 1A8, Canada

⁵Banting and Best Diabetes Centre, University of Toronto, Toronto, ON M5G 2C4, Canada

⁶Co-first author

⁷Present address: Faculty of Biological Sciences, School of Biomedical Science, University of Leeds, Leeds, LS2 9JT, UK

⁸Lead Contact

*Correspondence: tony.lam@uhnres.utoronto.ca

<http://dx.doi.org/10.1016/j.celrep.2017.02.035>

SUMMARY

Mitochondria undergo dynamic changes to maintain function in eukaryotic cells. Insulin action in parallel regulates glucose homeostasis, but whether specific changes in mitochondrial dynamics alter insulin action and glucose homeostasis remains elusive. Here, we report that high-fat feeding in rodents incurred adaptive dynamic changes in mitochondria through an increase in mitochondrial fission in parallel to an activation of dynamin-related protein 1 (Drp1) in the dorsal vagal complex (DVC) of the brain. Direct inhibition of Drp1 negated high-fat-feeding-induced mitochondrial fission, endoplasmic reticulum (ER) stress, and insulin resistance in the DVC and subsequently restored hepatic glucose production regulation. Conversely, molecular activation of DVC Drp1 in healthy rodents was sufficient to induce DVC mitochondrial fission, ER stress, and insulin resistance. Together, these data illustrate that Drp1-dependent mitochondrial fission changes in the DVC regulate insulin action and suggest that targeting the Drp1-mitochondrial-dependent pathway in the brain may have therapeutic potential in insulin resistance.

Mitochondria exist as dynamic organelles that undergo morphological changes in response to nutritional status. In response to nutrient shortage, mitochondria fuse to form elongated mitochondria so as to maximize ATP production, whereas during nutrient excess, they undergo fission to form smaller, fragmented mitochondrion, in order to prevent overt ATP synthesis (Mishra and Chan, 2016). Whereas mitofusin 1 and 2 and optic atrophy 1 are regulators of mitochondria fusion, the canonical mechanism of mitochondria fission is dependent on the dyna-

min-like protein, Drp1 (Mishra and Chan, 2016; Youle and van der Bliek, 2012). The role of mitochondrial dynamics in regulating cellular energy metabolism has been extensively studied, where changes in specific mitochondrial dynamic events have been implicated to alter cellular and whole-body homeostatic action of insulin.

For example, alteration of mitochondrial β -oxidation (Befroy et al., 2007) and density (Kelley et al., 2002; Morino et al., 2005) are associated with muscle insulin resistance in humans, whereas obese rodents and humans exhibit smaller mitochondria in the skeletal muscle (Jheng et al., 2012; Kelley et al., 2002). One study reports an increase in Drp1-dependent mitochondrial fission in the muscle associated with insulin resistance in rodents (Jheng et al., 2012) and another demonstrates that liver-specific mitofusin 2 knockdown mice are hepatic insulin resistant and glucose intolerant (Sebastián et al., 2012). Although the overall and relative contribution of mitochondrial fission and fusion in insulin resistance in rodents and humans is of emerging interest, it remains unclear whether changes in mitochondrial dynamism affect brain insulin action and consequently whole-body glucose regulation in vivo.

In this regard, insulin action in the hypothalamus and the dorsal vagal complex (DVC) of the brain lowers hepatic glucose production in healthy rodents but, when subjected to high-fat feeding as short as 3 days, is disrupted in both the brain regions (Filippi et al., 2012; Ono et al., 2008; Pocai et al., 2005). Activation of S6 kinase in parallel to an increase in hypothalamic inflammation is implicated in diet-induced hypothalamic insulin resistance (Ono et al., 2008; Thaler et al., 2012; Zhang et al., 2008). In the DVC, however, the potential mechanistic link(s) between high-fat feeding and insulin resistance remain elusive. Characterizing DVC insulin resistance warrants an urgent necessity, especially in light of the clinical findings that intranasal insulin delivery, which would target the hypothalamus and DVC, improves insulin sensitivity and lowers glucose production in healthy, but not obese, humans (Dash et al., 2015; Heni et al., 2014). We here focused on dissecting DVC insulin resistance in rodents and

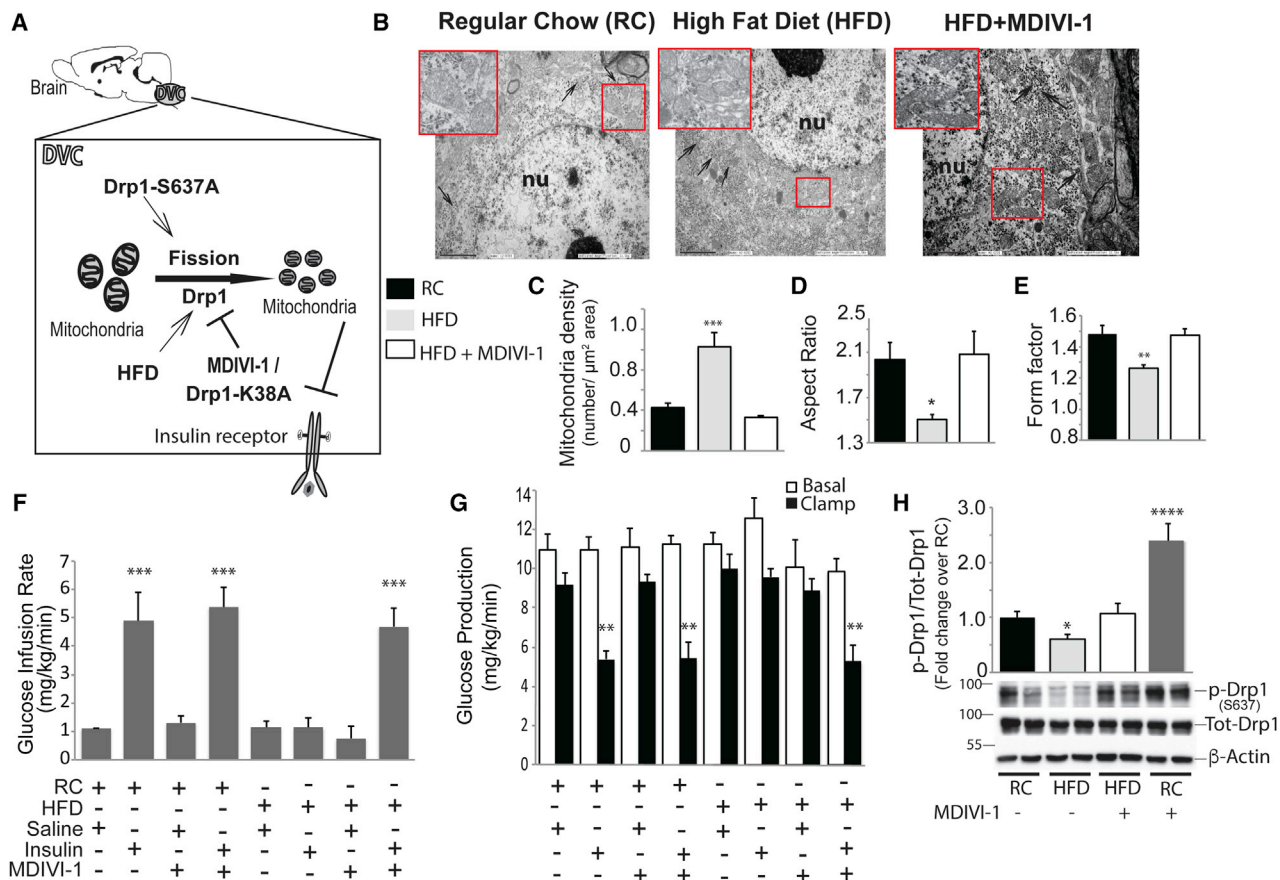


Figure 1. HFD Induces Mitochondrial Fission and Insulin Resistance in the DVC via Drp1

(A) Schematic representation of the working hypothesis.

(B) Representative electron microscopy images of mitochondria in the somatic regions of the DVC taken from RC, 3-day HFD, and 3-day HFD + DVC MDIVI-1-treated rats. The scale bar represents 2 μm; black arrow, rough endoplasmic reticulum; corner red square inset, enlarged image of mitochondria from the smaller red-boxed area; nu, nucleus.

(C) Mitochondria density from RC (144 mitochondria from nine neurons), 3-day HFD (287 mitochondria from eight neurons), and 3-day HFD+ DVC MDIVI-1 (104 mitochondria from six neurons)-treated rats.

(D) Aspect ratio from RC (141 mitochondria from nine neurons), 3-day HFD (238 mitochondria from eight neurons), and 3-day HFD+ DVC MDIVI-1 (97 mitochondria from six neurons)-treated rats.

(E) Form factor from RC (75 mitochondria from nine neurons), 3-day HFD (75 mitochondria from eight neurons), and 3-day HFD+ DVC MDIVI-1 (75 mitochondria from six neurons)-treated rats.

(F) Glucose infusion rate during the clamps.

(G) Glucose production in basal (white square) and clamp (black square) conditions.

n = 6 for saline RC rats, n = 8 for insulin RC rats, n = 5 for MDIVI-1 + saline RC rats, n = 5 for MDIVI-1 + insulin RC rats, n = 10 for insulin HFD rats, n = 4 for MDIVI-1 + saline HFD rats, and n = 7 for insulin + MDIVI-1 HFD rats. *p < 0.05; **p < 0.01; ***p < 0.001; ****p < 0.0001. Values are shown as mean + SEM.

(H) p-Drp1 levels (normalized to total-Drp1) in the DVC of RC (n = 16), HFD (n = 16), MDIVI-1 + HFD (n = 12), and MDIVI-1 + RC (n = 6) rats; representative western blot image pasted below.

See also [Figure S1](#) and [Tables S1](#) and [S2](#).

hypothesize that changes in mitochondria dynamics play a causative role in DVC insulin resistance ([Figure 1A](#)).

RESULTS

High-Fat Feeding Induces DVC Mitochondrial Fission and Insulin Resistance via Drp1

We obtained cross-sectional slides containing the DVC from rats fed a 3-day high-fat diet (HFD) or regular chow (RC) ([Figure S1A](#)).

Electron microscopy imaging in the somatic portions ([Figure 1B](#)) of DVC neuronal cells indicated that HFD versus RC increased the number of mitochondria in the neuronal soma (reflected by increased density of mitochondria per cell area; [Figure 1C](#)). These mitochondria were less elongated and elliptical (reflected by decreased aspect ratio; [Figure 1D](#)) and were shorter and less branched (reflected by decreased form factor; [Figure 1E](#)). Notably, no such differences in the mitochondrial density and morphology were observed in the dendritic compartments of

DVC neurons between HFD versus RC rats (Figures S1C–S1F). Given that the observed mitochondrial changes in the DVC neuronal cell bodies could either be due to an increase in fission or a decrease in fusion, we chose to first examine the role of the fission protein Drp1 in this process.

We inhibited DVC Drp1 via DVC infusion of Drp1 inhibitor MDIVI-1, which blocks Drp1 translocation from the cytosol to the mitochondria (Cassidy-Stone et al., 2008). The daily DVC MDIVI-1 infusion was administered 1 day after the initiation of HFD and maintained for 3 days (Figure S1A). Infusion of MDIVI-1 during HFD reversed the HFD-induced changes in the somatic mitochondrial morphology (Figure 1B) as the mitochondria density (Figure 1C), aspect ratio (Figure 1D), and form factor (Figure 1E) were normalized back to RC levels. The mitochondria in the dendrites remained unaffected by MDIVI-1 (Figures S1C–S1F). Thus, HFD alters Drp1 to induce mitochondrial fission in the DVC and raises the possibility that Drp1-dependent mitochondrial fission is necessary for HFD-induced DVC insulin resistance.

To address this, we first confirmed that infusion of insulin versus saline into the DVC of healthy rats increased exogenous glucose infusion rate (Figure 1F) needed to maintain euglycemia (Table S1) under pancreatic-(basal insulin) clamp conditions (Table S2; Figure S1B). The elevation in glucose infusion rate induced by DVC insulin infusion was due to an inhibition of glucose production (Figures 1G and S1G) and not an increase in glucose uptake (Figure S1H). The gluco-regulatory effect of DVC insulin was abolished in 3-day HFD rats (Figures 1F, 1G, S1G, and S1H; Tables S1 and S2), consistent with the previous report that HFD induces DVC insulin resistance (Filippi et al., 2012). Importantly, we here discovered that co-infusion of insulin with MDIVI-1 into the DVC, at a dose that MDIVI-1 negated 3-day HFD to increase mitochondrial fission (Figures 1B–1E), also restored DVC insulin to regulate glucose kinetics and specifically in lowering glucose production in 3-day HFD rats (Figures 1F, 1G, S1G, and S1H; Tables S1 and S2). In parallel, DVC MDIVI-1 infusion did not alter glucose regulation while insulin is infused into the DVC of RC-fed rats as compared to insulin alone (Figures 1F, 1G, S1G, and S1H; Table S1). These data indicate that inhibiting DVC Drp1-dependent mitochondrial fission selectively restores the ability of insulin to lower glucose production during HFD and demonstrate that Drp1-dependent mitochondrial fission in the DVC is necessary to induce brain insulin resistance.

To confirm HFD changes in Drp1, we next assessed the phosphorylation of Drp1 in the DVC of 3-day HFD rats and found a reduction of phosphorylated Drp1 (p-Drp1) in the residue S637 induced by HFD versus RC (Figure 1H). A decrease in pDrp1 (S637) increases Drp1 activity (Chang and Blackstone, 2007), thereby indicating that HFD activates DVC Drp1. DVC MDIVI-1 infusion normalized the reduced DVC p-Drp1 levels in HFD rats, comparable to RC (Figure 1H), whereas DVC MDIVI-1 infusion in RC rats increased p-Drp1 levels compared to RC without MDIVI-1 (Figure 1H).

Molecular Inhibition of Drp1 Reverses Mitochondrial Fission and HFD-Induced DVC Insulin Resistance

We next tested the effects of an adenoviral-mediated molecular inhibition of Drp1 in reversing HFD-induced DVC insulin resis-

tance. The adenoviral construct was driven by a cytomegalovirus (CMV) promoter expressing a FLAG-tagged dominant-negative form of Drp1 (Drp1 K38 to A [Drp1-KA]). The Drp1-KA lacks the guanosine triphosphate (GTP) binding site required for Drp1 (a GTPase) to carry out its mitochondrial fission activity. Although this approach was used to block Drp1 in *in vitro* and *in vivo* models (Qi et al., 2013; Rappold et al., 2014), in the current study, we first validated the virus in HEK293 cells and evaluated for potential changes in Drp1 localization and mitochondrial morphology in infected cells using confocal microscopy. Whereas mitochondrial translocation of Drp1 is a hallmark of mitochondrial fission, our co-localization analysis revealed that Drp1-KA-FLAG expression negatively correlated with mitochondrial staining in HEK293 cells, much less than the random co-localization observed for the GFP controls with mitochondria (Figure 2A), thereby indicating that the KA mutation indeed blocked Drp1 translocation to the mitochondria. Using z stack images, we then constructed a 3D model of individual cells (Movie S1) that were infected with Drp1-KA or GFP and found that Drp1-KA versus GFP reduced the number of mitochondria (Movie S1; Figure 2B) and altered mitochondria morphology indicated by an increase in aspect ratio (Figure 2C) and an increase in average mitochondria volume (Figure 2D). Thus, the overall effect of Drp1-KA expression was indeed an inhibition in mitochondrial fission.

We then injected the Drp1-KA-FLAG or GFP control virus into the DVC of HFD rats to examine whether Drp1-KA would alleviate DVC insulin resistance. We validated that Drp1-KA-FLAG was expressed only in the DVC, but not in the neighboring brain regions (Figures S2A and S2B), and evaluated the effect of Drp1-KA versus GFP on DVC insulin action during pancreatic clamps in 3-day HFD-fed rats (Figure S1B). DVC insulin infusion failed to increase glucose infusion rate and lower glucose production in GFP-injected HFD versus RC-fed rats (Figures 2E, 2F, and S2C). Consistent with the effects of MDIVI-1, Drp1-KA injection in rats was also protective against HFD-induced DVC insulin resistance in restoring the ability of DVC insulin to increase glucose infusion rate and lower glucose production (Figures 2E, 2F, and S2C). Drp1-KA did not alter insulin action in RC rats (Figures 2E, 2F, and S2C), and glucose uptake was comparable among groups (Figure S2D). Thus, DVC-targeted inhibition of Drp1 reverses HFD-induced insulin resistance.

Molecular Activation of Drp1 Induces Mitochondrial Fission and DVC Insulin Resistance

We evaluated whether activation of Drp1 *per se* was sufficient to induce insulin resistance. We generated an adenovirus driven by a CMV promoter expressing a FLAG-tagged phospho-deficient mutant of Drp1 (Drp1 S637 to A [Drp1-SA]), which is constitutively active, as a decrease in pDrp1 (S637) increases Drp1 activity (Chang and Blackstone, 2007). Using confocal microscopy, we assessed the potential co-localization between Drp1-SA-FLAG or GFP and mitochondria and evaluated for changes in mitochondria morphology in individual infected cells. We discovered that Drp1-SA-FLAG infection overlapped and positively correlated with some mitochondria in HEK293 cells compared to the random co-localization of control GFP with mitochondria in cells based on dual-color imaging (Figure 3A). Using z stack

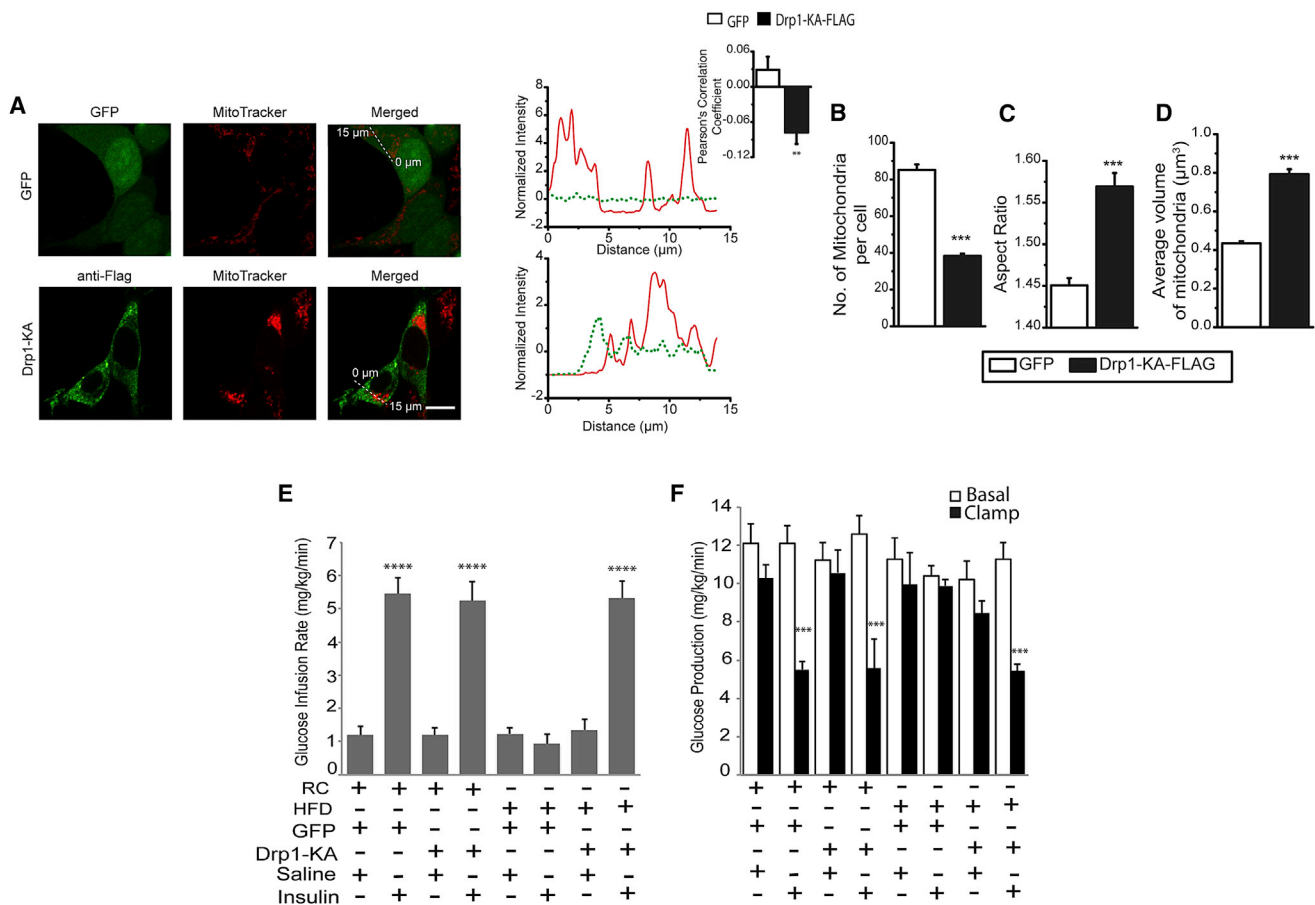


Figure 2. Drp1-KA Expression on Mitochondria Dynamics and Insulin Action

(A) Representative confocal microscopy images of HEK293 cells expressing GFP or Drp1-KA-FLAG (green). Mitochondria are stained with Mitotracker Red (red), and overlay images are shown. The scale bar represents 10 μm . The dashed white line on the merged image represents the analyzed region as shown to the right (0–15 μm). The line profiles indicate the intensity of Mitotracker Red and the GFP or Drp1-KA-FLAG. Pearson's correlation coefficient analysis is presented from 66 cells for GFP and 43 cells for Drp1-KA-FLAG.

(B) Number of mitochondria per cell.

(C) Aspect ratio of mitochondria.

(D) Average volume of mitochondria.

(B–D) Eighty-one cells for GFP and 81 cells for Drp1-KA were analyzed obtained from three independent experiments.

(E) Glucose infusion rate during the clamps of adenoviral-DVC-infected rats.

(F) Glucose production in basal (white square) and clamp (black square) conditions.

n = 6 for saline GFP RC, n = 10 for insulin GFP RC, n = 5 for saline Drp1-KA RC, n = 5 for insulin Drp1-KA RC, n = 6 for saline GFP HFD, n = 5 for saline Drp1-KA HFD and n = 5 for insulin Drp1-KA HFD rats. **p < 0.01; ***p < 0.001; ****p < 0.0001. Values are shown as mean + SEM. See also [Figure S2](#) and [Movie S1](#).

images, we then constructed the 3D model of individual cells ([Movie S2](#)) that were infected with Drp1-SA or GFP and found that Drp1-SA increased the number of mitochondria ([Movie S2](#); [Figure 3B](#)) and altered mitochondria morphology indicated by a reduction in aspect ratio ([Movie S2](#); [Figure 3C](#)) and mean mitochondrial volume ([Movie S2](#); [Figure 3D](#)). The overall effect of Drp1-SA is an increase in mitochondrial fission.

We next injected the adenovirus expressing Drp1-SA-FLAG or GFP into the DVC of RC rats ([Figure S1B](#)). Localization studies confirmed that Drp1-SA-FLAG was selectively expressed in the DVC, but not in the adjacent regions ([Figures S2A](#) and [S2E](#)) of the same rats. We then evaluated the effect of Drp1-SA versus GFP on insulin action in RC rats ([Figure S1B](#)) and found that,

although DVC insulin infusion in GFP rats was still able to increase glucose infusion rate to maintain euglycemia ([Figure 3E](#)) and lower glucose production ([Figures 3F](#) and [S2F](#)) with no changes in glucose uptake ([Figure S2G](#)), DVC insulin infusion failed to alter glucose kinetics in Drp1-SA rats ([Figures 3E](#), [3F](#), [S2F](#), and [S2G](#)). Hence, molecular activation of Drp1-dependent mitochondria in the DVC was sufficient to induce insulin resistance and recapitulate the effect of HFD.

Drp1-Dependent Mitochondrial Fission Enhances ER-Stress-Dependent Insulin Resistance in the DVC

Drp1-dependent mitochondrial fission in the pancreatic β cells elevates endoplasmic reticulum (ER) stress ([Peng et al., 2011](#))

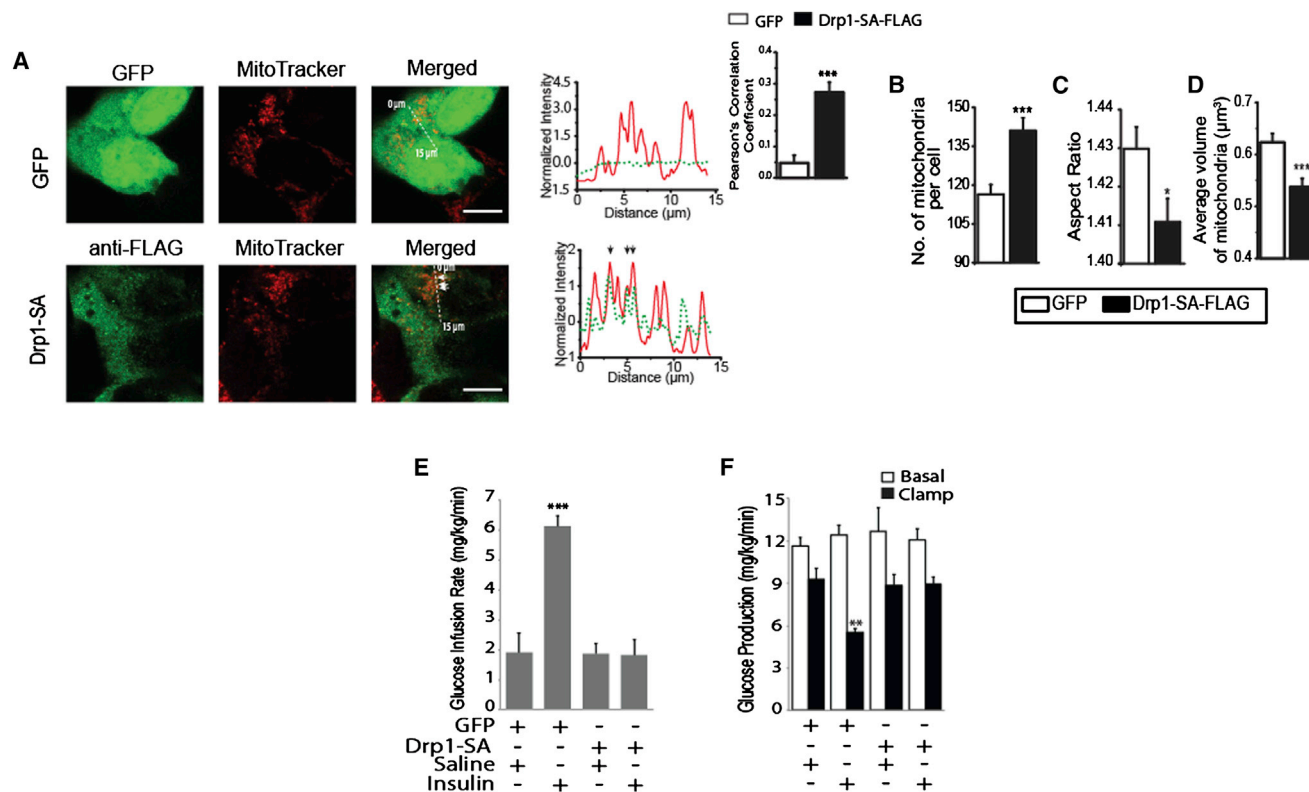


Figure 3. Drp1-SA Expression on Mitochondria Dynamics and Insulin Action

(A) Representative confocal microscopy images of HEK293 cells expressing GFP or Drp1-SA-FLAG (green). Mitochondria are stained with Mitotracker Red (red), and overlay images are shown. The scale bar represents 10 μm. The dashed white line on the merged image represents the analyzed region as shown to the right (0–15 μm). The line profiles indicate the intensity of Mitotracker Red and the GFP or Drp1-SA-FLAG. Overlapping region is indicated by an arrow. Pearson's correlation coefficient analysis is presented from 60 cells for GFP and 55 cells for Drp1-SA-FLAG.

(B) Number of mitochondria per cell.

(C) Aspect ratio of mitochondria.

(D) Average volume of mitochondria.

(B–D) Eighty-nine cells for GFP and 83 cells for Drp1-SA were analyzed and obtained from three independent experiments.

(E) Glucose infusion rate during the clamps of adenoviral-DVC-infected rats.

(F) Glucose production in basal (white square) and clamp (black square) conditions.

n = 5 for saline GFP rats, n = 6 for insulin GFP rats, saline Drp1-SA rats, and insulin Drp1-SA rats. *p < 0.05; **p < 0.01; ***p < 0.001. Values are shown as mean + SEM. See also [Figure S2](#) and [Movie S2](#).

and mediates fatty-acid-induced ER expansion (Wikstrom et al., 2013). In parallel, elevated ER stress induces hepatic (Yang et al., 2015) and hypothalamic insulin resistance (Zhang et al., 2008). Thus, we here evaluated whether ER stress mediates the ability of HFD-induced Drp1-dependent mitochondria changes in the DVC to impair insulin action (Figure 4A). We first found that 3-day HFD versus RC increased ER stress marker p-PERK (T980) in the DVC (Figures 4B and S1A). This effect of HFD on p-PERK was negated by DVC ER stress inhibitor 4-phenylbutyrate (4-PBA) infusion (Figure 4B) and recapitulated by DVC ER stress inducer tunicamycin (TM) administration (Figures 4C and S1A). Co-infusion of 4-PBA with insulin into the DVC of 3-day HFD rats restored the ability of DVC insulin to increase glucose infusion rate (Figure 4D) and lower glucose production (Figure 4E) to a comparable extent as DVC insulin-infused RC rats (Figures 4D and 4E), whereas DVC 4-PBA infusion alone did not alter glucose kinetics (Figures 4D and 4E). Conversely, DVC TM infu-

sion was sufficient to induce DVC insulin resistance (Figures 4D and 4E) but, when infused alone without insulin, did not alter glucose kinetics (Figures 4D and 4E). Glucose uptake was comparable among groups (Figure S3A). Thus, ER stress in the DVC is necessary for HFD and sufficient to induce insulin resistance.

We evaluated whether ER stress is necessary for mitochondrial fission to induce insulin resistance (Figure 4A). We first found that DVC 4-PBA infusion failed to prevent the ability of HFD to decrease p-Drp1 (or activate Drp1; Figures 4F and S1A), whereas DVC MDIVI-1 infusion negated the ability of HFD to increase p-PERK (Figure 4G). Together with the fact that DVC 4-PBA negated HFD to increase ER stress (Figure 4B) and DVC MDIVI-1 prevented HFD-induced mitochondrial fission (Figures 1B–1E), these data demonstrate that ER stress is a downstream effector of HFD-induced Drp1-dependent mitochondrial fission in the DVC. Consistently, activation of Drp1-dependent mitochondrial fission in the DVC via DVC Drp1-SA

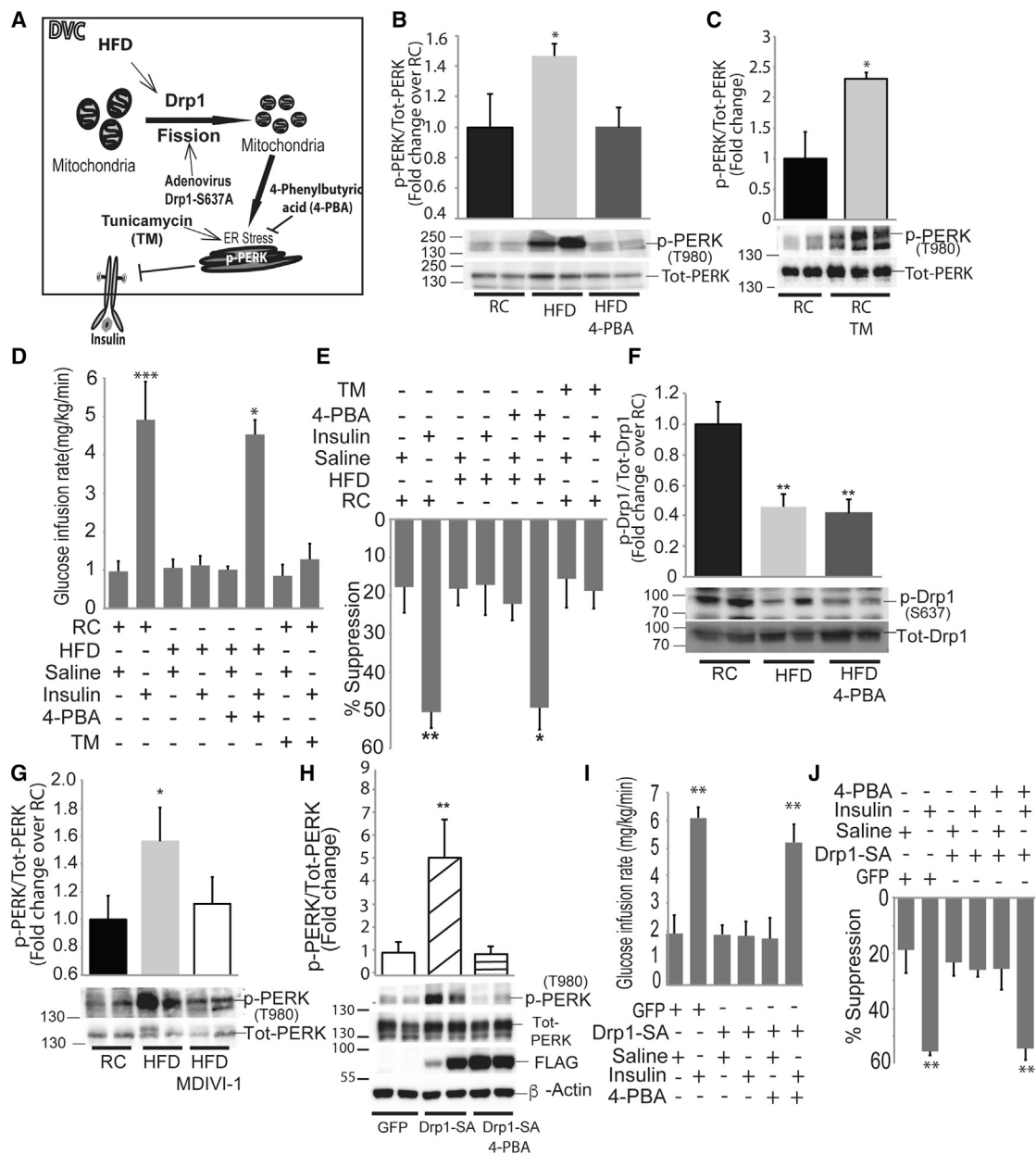


Figure 4. Drp1-Mitochondrial Fission Enhances ER-Stress-Dependent DVC Insulin Resistance

(A) Schematic representation of the working hypothesis.

(B and C) DVC ER-stress marker PERK phosphorylation (T980) levels were analyzed and normalized to total PERK with representative western blot image pasted below. $n = 5$ for RC and HFD and $n = 6$ for HFD + 4-PBA rats (B); $n = 12$ for RC and $n = 6$ for TM rats (C).

(D) Glucose infusion rate during the clamp.

(E) Glucose production suppression expressed as the percentage reduction from basal (60–90 min) to clamp (final 30 min) conditions. $n = 6$ for saline RC, $n = 8$ for insulin RC, $n = 7$ for saline HFD, $n = 10$ for insulin HFD, $n = 5$ for 4-PBA + saline or 4-PBA + insulin HFD, $n = 6$ for saline + TM RC, and $n = 5$ for RC insulin + TM rats.

(F) p-Drp1 levels (normalized to total-Drp1) in the DVC of RC ($n = 5$), HFD ($n = 6$), and HFD + 4-PBA ($n = 6$) rats with representative western blot image pasted below.

(G and H) DVC ER-stress marker PERK phosphorylation (T980) levels were analyzed and normalized to total PERK with representative western blot image pasted below. $n = 9$ for RC, $n = 14$ for HFD, and $n = 13$ for HFD + MDIVI-1 rats (G); $n = 5$ for GFP, $n = 4$ for Drp1-SA, and $n = 5$ for Drp1-SA + 4-PBA rats (H).

(I) Glucose infusion rate during the clamps of adenoviral-DVC-infected rats.

(J) Glucose production suppression expressed as the percentage reduction from basal (60–90 min) to clamp (final 30 min) conditions.

$n = 6$ for saline GFP, $n = 6$ for insulin GFP, $n = 6$ for saline Drp1-SA or insulin Drp1-SA or insulin + 4-PBA-Drp1-SA rats, and $n = 5$ for saline + 4-PBA-Drp1-SA rats.

* $p < 0.05$; ** $p < 0.01$; *** $p < 0.001$. Values are shown as mean + SEM. See also Figure S3.

injection induced ER stress (Figure 4H) and insulin resistance (Figures 4I and 4J) in RC rats. DVC 4-PBA infusion in Drp1-SA rats reduced ER stress (Figures 4H and S1A) and restored the ability of DVC insulin infusion to increase glucose infusion rate (Figure 4I) and lower glucose production (Figure 4J) with no changes on glucose uptake (Figure S3B). DVC 4-PBA infusion alone, independent of insulin co-infusion, did not alter glucose kinetics in DVC Drp1-SA rats (Figures 4I, 4J, and S3B). Thus, HFD-induced DVC Drp1-dependent mitochondrial fission elevates ER stress and subsequently induces insulin resistance.

An induction of inducible nitric oxide synthase (iNOS) expression in the muscle by HFD induces insulin resistance (Perreault and Marette, 2001) and, in the liver, mediates HFD-induced S-nitrosylation to elevate ER stress and impair insulin signaling (Yang et al., 2015). An activation of Drp1-dependent mitochondrial fission by lipopolysaccharide elevates iNOS in microglial cells as well (Park et al., 2013). This led us to hypothesize that an increase in iNOS could mediate the ability of Drp1-dependent mitochondrial fission to induce insulin resistance. To begin addressing this possibility, we first infected PC12 cells with the Drp1-SA-FLAG virus that induced ER stress (Figure 4H) and insulin resistance (Figures 4I and 4J) and found that Drp1-SA versus GFP increased iNOS (Figure S4A). Moreover, Drp1-SA versus GFP viral injection into the DVC of RC rats also increased DVC iNOS expression (Figure S4B). In parallel, 3-day HFD increased DVC iNOS expression (Figure S4C) and such effect was negated by DVC MDIVI-1 (Figure S4C). These findings preliminarily indicate that Drp1-dependent mitochondrial fission is necessary for HFD and sufficient to increase iNOS expression. Together with the fact that ER stress is required for elevated iNOS expression in the liver to induce insulin resistance (Yang et al., 2015) and for Drp1-dependent mitochondrial fission in the DVC to induce insulin resistance (Figures 4I and 4J), we put forward a working hypothesis that an iNOS-ER stress axis in the brain is necessary for HFD-induced Drp1-dependent mitochondrial fission to induce insulin resistance.

The insulin signaling pathway is negatively regulated by serine phosphorylation of insulin receptor substrate (IRS) (Capps and White, 2012). In addition, mitochondria dysfunction and ER stress have been linked to an increase in serine IRS1 phosphorylation in muscle and liver (Morino et al., 2005; Ozcan et al., 2004). To finally assess whether HFD-induced DVC Drp1-dependent mitochondrial fission impairs insulin action, we assessed the serine phosphorylation status of IRS1 in the DVC in HFD rats. We discovered that 3-day HFD increased phosphorylation of IRS1 Ser-1101 (IRS1-p-S1101) (Figure S4D), consistent with the fact that hepatic IRS1-p-S1101 is elevated in obese rodents (Tremblay et al., 2007). DVC MDIVI-1 infusion in 3-day HFD rats that inhibited Drp1-dependent mitochondrial fission (Figures 1B–1E), iNOS expression (Figure S4C), and ER stress (Figure 4G) also negated the ability of HFD to increase IRS1-p-S1101 (Figure S4D), confirming that an increase in DVC mitochondrial fission induces insulin resistance.

DISCUSSION

Our discoveries indicate that activation of Drp1-mitochondrial fission in the DVC is sufficient and necessary for HFD to elevate

ER stress and iNOS and induce insulin resistance in rodents. Together with the fact that iNOS and ER stress mediates hepatic and muscle insulin resistance (Perreault and Marette, 2001; Yang et al., 2015), inhibiting whole-body Drp1 reverses muscle insulin resistance in obese rodents (Jheng et al., 2012), and exercise increases insulin sensitivity in association to a decrease in muscle Drp1 in obese and insulin-resistant humans (Fealy et al., 2014), mitochondrial fission may represent a primary and fundamental process in insulin-sensitive organs that govern insulin action. Nonetheless, the mechanistic and causative sequential link of Drp1-mitochondrial fission, ER stress, and iNOS to insulin resistance in the brain, as well as the underlying neurocircuitry involved, warrant future investigation.

The metabolic impact of brain-specific changes in mitochondrial dynamics is becoming apparent as manipulation of mitochondria dynamics in neurons alters the progression of obesity and metabolic status in rodents (Schneeberger et al., 2013; Dietrich et al., 2013; Toda et al., 2016). Our current set of data not only strengthens the claim that changes in brain mitochondrial dynamics impact whole-body metabolic regulation but also specifically demonstrates that bi-directional changes of Drp1-mitochondrial fission in the DVC regulate insulin action in vivo. Further, these findings support the notion that HFD increases mitochondrial fission and ER stress that leads to brain insulin and leptin resistance (Schneeberger et al., 2013; Zhang et al., 2008).

How high-fat feeding affects mitochondrial fission in the somatic portions of neurons versus dendrites is yet to be answered. Interestingly, studies from the Alzheimer's disease field report that mitochondrial fission/fusion proteins and other mitochondrial membrane proteins, such as COX1 and mtDNA, show a pattern of redistribution away from neuronal processes to only soma in the hippocampal neurons of a brain affected by Alzheimer's (Wang et al., 2009). The distinct neuronal populations involved in displaying the HFD-induced changes in mitochondria fission, and possibly redistribution to soma in the DVC to induce insulin resistance, remain largely unknown and an important future research direction.

Our findings also open the question of how Drp1 is activated in response to HFD. We hypothesize that serine threonine phosphatase calcineurin, which dephosphorylates Drp1 S637, may be the mediator as calcineurin increases Drp1-mitochondrial fission during ischemia-reperfusion injury in cardiomyocytes (Sharp et al., 2014), whereas increased calcineurin activity in neurons mediate mitochondrial translocation of Drp1 and cause mitochondrial fragmentation in Huntington's disease (Costa et al., 2010). Further, a knockdown of muscle calcineurin hyperphosphorylated Drp1 and increased mitochondrial elongation (Pfluger et al., 2015). Whether DVC calcineurin ablation would prevent the HFD-induced decrease in p-Drp1 levels, increase in mitochondrial fission, and induction of insulin resistance merits future investigation. In parallel, AMPK activation is linked to mitochondrial fission (Toyama et al., 2016). Given that an inhibition of hypothalamic AMPK lowers glucose production (Yang et al., 2010), we postulate that an AMPK-Drp1-dependent mitochondrial fission in the DVC regulates insulin action. In summary, we postulate that targeting the Drp1-mitochondria-dependent pathways in the brain may carry therapeutic potential to reverse insulin resistance in metabolic disorders.

EXPERIMENTAL PROCEDURES

All study protocols were approved by the UHN Animal Care and Use Committee.

Animal Preparation

Eight-week-old male Sprague-Dawley (SD) rats weighing between 260 and 280 g (Charles River Laboratories) were used. Rats were housed in individual cages and maintained on a standard light-dark cycle with access to chow (RC) diet and water ad libitum.

In one set of experiments (Figure S1A), rats were stereotactically (David Kopf Instruments) implanted with indwelling bilateral catheters targeting the nucleus of the solitary tract (NTS) within the DVC (0.0 mm on occipital crest, 0.4 mm lateral to midline, and 7.9 mm below skull surface; Filippi et al., 2012) on day 0. After 1 week of recovery, rats were given either Lard oil-enriched HFD or RC for 3 days (Figure S1A). The diet composition for RC (3.1 kcal/g) was 18% fat, 49% carbohydrate, and 33% protein (Teklad diet 7002 from Harlan Laboratories) or HFD (3.9 kcal/g) was 34% fat, 44% carbohydrate, and 22% protein (modified lab with 10% lard 571R diet from TestDiet). On days 8 and 9, the HFD rats received 2 μ L infusion of MDIVI-1 (100 μ M) or saline. On day 10 (after a 4- to 6-hr fast), an infusion of MDIVI-1 (100 μ M) or saline was given at 0.006 μ L/min for 270 min into the DVC. The concentration of 100 μ M MDIVI-1 was chosen based on the half maximal inhibitory concentration (IC_{50}) of MDIVI-1 (10 μ M; Cassidy-Stone et al., 2008) and factoring into a dilution factor when chemical inhibitors are DVC infused. The rats were then subjected to a cardiac perfusion with a solution of 2% glutaraldehyde in 0.1 M sodium cacodylate buffer and received an injection of 3 μ L bromophenol blue through each side of the bilateral DVC catheter to verify the correct placement of the catheters. The DVC (see Figure S2A) was then collected and processed for electron microscopy analysis. Alternatively, the rats were immediately sacrificed and DVC brain region was validated via bromophenol blue and collected for western blot analysis.

Pancreatic-Euglycemic Clamp, Glucose Kinetics Analysis, and Brain Tissues Sampling

In a parallel set of studies, rats were stereotactically implanted with indwelling DVC. After 1 week of recovery, rats underwent intravenous catheterization where the internal jugular vein and carotid artery were catheterized for infusion and sampling and were placed either on RC or HFD (Figure S1B). Four days post-intravenous catheterization, rats whose food intake and body weight had recovered back to within 10% of baseline underwent the studies. Rats were fasted 4–6 hr before the clamp experiments (Figure S1B). Insulin (a total of 2.52 μ U; 1.26 μ U per site) or saline was infused at 0.006 μ L/min (from time 0 to 210) through the DVC catheters (Filippi et al., 2012). MDIVI-1 (100 μ M) or 4-PBA (5.4 μ g/ μ L) was pre-infused at 0.006 μ L/min for 1 hr (time –60) into the DVC and infused or co-infused with insulin during the clamp. ER stress inducer TM (0.033 μ g/ μ L) was pre-infused at 0.006 μ L/min for 4 hr before and then was infused throughout the clamp (Figure S1B). We have validated that 4-PBA and TM infused into the DVC bi-directionally and respectively alters p-PERK/total PERK (Figures 4B and 4C). A primed continuous intravenous infusion of [3 -H]-glucose (40 μ Ci bolus; 0.4 μ Ci/min) was initiated at 0 min and maintained throughout the study to assess glucose kinetics. A pancreatic (basal insulin)-euglycemic clamp was initiated at time 90 min and lasted until 210 min. Somatostatin (3 μ g/kg/min) was infused intravenously along with insulin (1.2 mU/kg/min) to replace plasma insulin levels back to basal. A 25% glucose solution was started at time 90 and periodically adjusted to maintain euglycemia. Samples for the determination of [3 -H]-glucose-specific activity and insulin levels were obtained at 10-min intervals. At the end of the experiments, rats were injected with 3 μ L bromophenol blue through each side of the bilateral DVC catheter to verify the correct placement of the catheter for the viral injection studies, whereas bromophenol blue was co-infused with chemical reagents for the non-viral injection studies (Figure S1B). Once the whole brain is harvested from the anesthetized rat via decapitation, the cerebellum is lifted to expose the caudal part of the brain (Figure S2A). Only those data for rats that showed injection of dye within the vagal triangle (Figure S2A, i and ii) were included. A spatula was used to extract the section of vagal triangle overlying the DVC (blue; Figure S2A, i and ii). In addition, sections of tissues were

dissected out from the left (yellow) regions of the caudal brain containing sp5 (spinal trigeminal tr.), Sp5C (spinal 5nu; caudal part), Sp5I (spinal 5nu; interolar), as well as from the region below the DVC (green) containing IN (12-hypoglossal nucleus), Ro (nucleus of roller), and InM (intermedius nucleus medulla; Figure S2A, iv–vi). Cerebellum (red; Figure S2A, i and iv–vi) and the mediobasal hypothalamus (pink) were also taken (Figure S2A, iii) for subsequent western blot analysis (Figures S2B and S2E).

Electron microscopy analysis of mitochondrion, western blotting, preparation and injection of Drp1-KA and Drp1-SA adenovirus in rats, HEK293 and PC12 expression of Drp1-KA and Drp1-SA and immunofluorescence, confocal imaging, mitochondrial morphology analysis, biochemical analysis, and statistical methods are described in detail in Supplemental Experimental Procedures.

SUPPLEMENTAL INFORMATION

Supplemental Information includes Supplemental Experimental Procedures, four figures, two tables, and two movies and can be found with this article online at <http://dx.doi.org/10.1016/j.celrep.2017.02.035>.

AUTHOR CONTRIBUTIONS

B.M.F. and M.A.A. conducted and designed the experiments, performed the data analyses, and wrote the manuscript. P.N.S., M.R., M.P.L., P.V.B., and J.V.R. assisted with the experiments. T.K.T.L. supervised the project, designed the experiments, and edited the manuscript.

ACKNOWLEDGMENTS

This work is supported by the Canadian Diabetes Association (OG-3-15-4901-TL) to T.K.T.L. and Natural Sciences and Engineering Research Council (NSERC) (RGPIN-2016-06468-JR) to J.V.R. M.A.A. is supported by a Canadian Institutes of Health Research (CIHR) doctoral award. P.N.S. is supported by a NSERC doctoral award. M.P.L. was supported by a CIHR graduate scholarship. P.V.B. is supported by an Ontario Graduate scholarship and a Banting and Best Diabetes Centre graduate scholarship. T.K.T.L. holds the John Kitson McIvor (1915–1942) Endowed Chair in Diabetes Research and the Canada Research Chair in Obesity at the Toronto General Hospital Research Institute and the University of Toronto.

Received: July 13, 2016

Revised: January 26, 2017

Accepted: February 11, 2017

Published: March 7, 2017

REFERENCES

- Befroy, D.E., Petersen, K.F., Dufour, S., Mason, G.F., de Graaf, R.A., Rothman, D.L., and Shulman, G.I. (2007). Impaired mitochondrial substrate oxidation in muscle of insulin-resistant offspring of type 2 diabetic patients. *Diabetes* 56, 1376–1381.
- Cassidy-Stone, A., Chipuk, J.E., Ingeman, E., Song, C., Yoo, C., Kuwana, T., Kurth, M.J., Shaw, J.T., Hinshaw, J.E., Green, D.R., and Nunnari, J. (2008). Chemical inhibition of the mitochondrial division dynamin reveals its role in Bax/Bak-dependent mitochondrial outer membrane permeabilization. *Dev. Cell* 14, 193–204.
- Chang, C.R., and Blackstone, C. (2007). Cyclic AMP-dependent protein kinase phosphorylation of Drp1 regulates its GTPase activity and mitochondrial morphology. *J. Biol. Chem.* 282, 21583–21587.
- Copps, K.D., and White, M.F. (2012). Regulation of insulin sensitivity by serine/threonine phosphorylation of insulin receptor substrate proteins IRS1 and IRS2. *Diabetologia* 55, 2565–2582.
- Costa, V., Giacomello, M., Hudec, R., Lopreiato, R., Ermak, G., Lim, D., Malorni, W., Davies, K.J., Carafoli, E., and Scorrano, L. (2010). Mitochondrial fission and cristae disruption increase the response of cell models of Huntington's disease to apoptotic stimuli. *EMBO Mol. Med.* 2, 490–503.

- Dash, S., Xiao, C., Morgantini, C., Koulajian, K., and Lewis, G.F. (2015). Intranasal insulin suppresses endogenous glucose production in humans compared with placebo in the presence of similar venous insulin concentrations. *Diabetes* *64*, 766–774.
- Dietrich, M.O., Liu, Z.W., and Horvath, T.L. (2013). Mitochondrial dynamics controlled by mitofusins regulate AgRP neuronal activity and diet-induced obesity. *Cell* *155*, 188–199.
- Fealy, C.E., Mulya, A., Lai, N., and Kirwan, J.P. (2014). Exercise training decreases activation of the mitochondrial fission protein dynamin-related protein-1 in insulin-resistant human skeletal muscle. *J. Appl. Physiol.* (1985) *117*, 239–245.
- Filippi, B.M., Yang, C.S., Tang, C., and Lam, T.K. (2012). Insulin activates Erk1/2 signaling in the dorsal vagal complex to inhibit glucose production. *Cell Metab.* *16*, 500–510.
- Heni, M., Wagner, R., Kullmann, S., Veit, R., Mat Husin, H., Linder, K., Benken-dorff, C., Peter, A., Stefan, N., Häring, H.U., et al. (2014). Central insulin administration improves whole-body insulin sensitivity via hypothalamus and parasympathetic outputs in men. *Diabetes* *63*, 4083–4088.
- Jheng, H.F., Tsai, P.J., Guo, S.M., Kuo, L.H., Chang, C.S., Su, I.J., Chang, C.R., and Tsai, Y.S. (2012). Mitochondrial fission contributes to mitochondrial dysfunction and insulin resistance in skeletal muscle. *Mol. Cell. Biol.* *32*, 309–319.
- Kelley, D.E., He, J., Menshikova, E.V., and Ritov, V.B. (2002). Dysfunction of mitochondria in human skeletal muscle in type 2 diabetes. *Diabetes* *51*, 2944–2950.
- Mishra, P., and Chan, D.C. (2016). Metabolic regulation of mitochondrial dynamics. *J. Cell Biol.* *212*, 379–387.
- Morino, K., Petersen, K.F., Dufour, S., Befroy, D., Frattini, J., Shatzkes, N., Nesch, S., White, M.F., Bilz, S., Sono, S., et al. (2005). Reduced mitochondrial density and increased IRS-1 serine phosphorylation in muscle of insulin-resistant offspring of type 2 diabetic parents. *J. Clin. Invest.* *115*, 3587–3593.
- Ono, H., Poci, A., Wang, Y., Sakoda, H., Asano, T., Backer, J.M., Schwartz, G.J., and Rossetti, L. (2008). Activation of hypothalamic S6 kinase mediates diet-induced hepatic insulin resistance in rats. *J. Clin. Invest.* *118*, 2959–2968.
- Ozcan, U., Cao, Q., Yilmaz, E., Lee, A.H., Iwakoshi, N.N., Ozdelen, E., Tuncman, G., Görgün, C., Glimcher, L.H., and Hotamisligil, G.S. (2004). Endoplasmic reticulum stress links obesity, insulin action, and type 2 diabetes. *Science* *306*, 457–461.
- Park, J., Choi, H., Min, J.S., Park, S.J., Kim, J.H., Park, H.J., Kim, B., Chae, J.I., Yim, M., and Lee, D.S. (2013). Mitochondrial dynamics modulate the expression of pro-inflammatory mediators in microglial cells. *J. Neurochem.* *127*, 221–232.
- Peng, L., Men, X., Zhang, W., Wang, H., Xu, S., Xu, M., Xu, Y., Yang, W., and Lou, J. (2011). Dynamin-related protein 1 is implicated in endoplasmic reticulum stress-induced pancreatic β -cell apoptosis. *Int. J. Mol. Med.* *28*, 161–169.
- Perreault, M., and Marette, A. (2001). Targeted disruption of inducible nitric oxide synthase protects against obesity-linked insulin resistance in muscle. *Nat. Med.* *7*, 1138–1143.
- Pfluger, P.T., Kabra, D.G., Aichler, M., Schriever, S.C., Pfuhlmann, K., García, V.C., Lehti, M., Weber, J., Kutschke, M., Rozman, J., et al. (2015). Calcineurin links mitochondrial elongation with energy metabolism. *Cell Metab.* *22*, 838–850.
- Poci, A., Lam, T.K., Gutierrez-Juarez, R., Obici, S., Schwartz, G.J., Bryan, J., Aguilar-Bryan, L., and Rossetti, L. (2005). Hypothalamic K(ATP) channels control hepatic glucose production. *Nature* *434*, 1026–1031.
- Qi, X., Qvit, N., Su, Y.C., and Mochly-Rosen, D. (2013). A novel Drp1 inhibitor diminishes aberrant mitochondrial fission and neurotoxicity. *J. Cell Sci.* *126*, 789–802.
- Rappold, P.M., Cui, M., Grima, J.C., Fan, R.Z., de Mesy-Bentley, K.L., Chen, L., Zhuang, X., Bowers, W.J., and Tieu, K. (2014). Drp1 inhibition attenuates neurotoxicity and dopamine release deficits in vivo. *Nat. Commun.* *5*, 5244.
- Schneeberger, M., Dietrich, M.O., Sebastián, D., Imbernón, M., Castaño, C., García, A., Esteban, Y., Gonzalez-Franquesa, A., Rodríguez, I.C., Bortolozzi, A., et al. (2013). Mitofusin 2 in POMC neurons connects ER stress with leptin resistance and energy imbalance. *Cell* *155*, 172–187.
- Sebastián, D., Hernández-Alvarez, M.I., Segalés, J., Soriano, E., Muñoz, J.P., Sala, D., Waget, A., Liesa, M., Paz, J.C., Gopalacharyulu, P., et al. (2012). Mitofusin 2 (Mfn2) links mitochondrial and endoplasmic reticulum function with insulin signaling and is essential for normal glucose homeostasis. *Proc. Natl. Acad. Sci. USA* *109*, 5523–5528.
- Sharp, W.W., Fang, Y.H., Han, M., Zhang, H.J., Hong, Z., Banathy, A., Morrow, E., Ryan, J.J., and Archer, S.L. (2014). Dynamin-related protein 1 (Drp1)-mediated diastolic dysfunction in myocardial ischemia-reperfusion injury: therapeutic benefits of Drp1 inhibition to reduce mitochondrial fission. *FASEB J.* *28*, 316–326.
- Thaler, J.P., Yi, C.X., Schur, E.A., Guyenet, S.J., Hwang, B.H., Dietrich, M.O., Zhao, X., Sarruf, D.A., Izgur, V., Maravilla, K.R., et al. (2012). Obesity is associated with hypothalamic injury in rodents and humans. *J. Clin. Invest.* *122*, 153–162.
- Toda, C., Kim, J.D., Impellizzeri, D., Cuzzocrea, S., Liu, Z.W., and Diano, S. (2016). UCP2 Regulates Mitochondrial Fission and Ventromedial Nucleus Control of Glucose Responsiveness. *Cell* *164*, 872–883.
- Toyama, E.Q., Herzig, S., Courchet, J., Lewis, T.L., Jr., Losón, O.C., Hellberg, K., Young, N.P., Chen, H., Polleux, F., Chan, D.C., and Shaw, R.J. (2016). Metabolism. AMP-activated protein kinase mediates mitochondrial fission in response to energy stress. *Science* *351*, 275–281.
- Tremblay, F., Brûlé, S., Hee Um, S., Li, Y., Masuda, K., Roden, M., Sun, X.J., Krebs, M., Polakiewicz, R.D., Thomas, G., and Marette, A. (2007). Identification of IRS-1 Ser-1101 as a target of S6K1 in nutrient- and obesity-induced insulin resistance. *Proc. Natl. Acad. Sci. USA* *104*, 14056–14061.
- Wang, X., Su, B., Lee, H.G., Li, X., Perry, G., Smith, M.A., and Zhu, X. (2009). Impaired balance of mitochondrial fission and fusion in Alzheimer's disease. *J. Neurosci.* *29*, 9090–9103.
- Wikstrom, J.D., Israeli, T., Bachar-Wikstrom, E., Swisa, A., Ariav, Y., Waiss, M., Kaganovich, D., Dor, Y., Cerasi, E., and Leibowitz, G. (2013). AMPK regulates ER morphology and function in stressed pancreatic β -cells via phosphorylation of DRP1. *Mol. Endocrinol.* *27*, 1706–1723.
- Yang, C.S., Lam, C.K., Chari, M., Cheung, G.W., Kokorovic, A., Gao, S., Leclerc, I., Rutter, G.A., and Lam, T.K. (2010). Hypothalamic AMP-activated protein kinase regulates glucose production. *Diabetes* *59*, 2435–2443.
- Yang, L., Calay, E.S., Fan, J., Arduini, A., Kunz, R.C., Gygi, S.P., Yalcin, A., Fu, S., and Hotamisligil, G.S. (2015). Metabolism. S-Nitrosylation links obesity-associated inflammation to endoplasmic reticulum dysfunction. *Science* *349*, 500–506.
- Youle, R.J., and van der Bliek, A.M. (2012). Mitochondrial fission, fusion, and stress. *Science* *337*, 1062–1065.
- Zhang, X., Zhang, G., Zhang, H., Karin, M., Bai, H., and Cai, D. (2008). Hypothalamic IKK β /NF- κ B and ER stress link overnutrition to energy imbalance and obesity. *Cell* *135*, 61–73.